MRI AND BIDIMENSIONAL RELAXOMETRY SEQUENCES FOR MACRO AND MICROSTRUCTURE ASSESSMENT IN FOOD MODELS

A.Melado-Herreros[1], P.Barreiro[1], M.E. Fernandez-Valle[2], T. Jimenez-Ariza[1], E.C. Correa[1], N. Campos[1], V. Diaz-Barcos[3], E.M. Rivas[4], M.I. Silóinz[4], B. Hills[5]

[1]LPF-TAGRALIA, UPM-CEI Moncloa. ETSI Agrónomos, Avda Complutense s/n. 28040, Madrid, Spain angela.melado@upm.es
[2]CAI NMR, Universidad Complutense de Madrid. Avda. Juan XXIII 1. 28040, Madrid, Spain
[3]EUIT Agrícola. UPM-CEI Moncloa. UPM. Avda Complutense s/n. 28040. Madrid, Spain.
[4]Department of Microbiology, Faculty of Biology, UCM_CEI Moncloa. C/José Antonio Novais, 12, 28040, Madrid, Spain
[5]Institue of Food Research. Norwich Research Park, Colney, NR4 7UA Norwich, UK

1 INTRODUCTION

Physico-chemical and organoleptic characteristics of food depend largely on the microscopic level distribution of gases, water, and connectivity and mobility through the pores[1,2] . Food microstructure is related to texture, microbiological stability[1,3], the in-mouth sensation perceived by the consumers[4], and also to nutritional properties. Nutrients might be located in natural cellular compartments and thus, microstructure may affect the final uptake of nutrients[5] . Several authors have studied microstructure of foods in order to a better understanding of several food technology processes, such as fruit and vegetable dehydration[6,7], study of internal disorders in fruits[8], the modelling of foods in order to have a better comprehension of their behaviour[9,10,11,12] or the microstructural changes of coffee during roasting[13].

(Micro)-structural characterization of food by non-invasive techniques can be accomplished by Magnetic Resonance Imaging (MRI)[14] and Nuclear Magnetic Spectroscopy (NMR)[1,15,16,17], combined with the application of methods of dissemination and multidimentional relaxometry[18,19, 20].

In this work, several artificial food models have been used, based on foamed gels, in order to study macro and microstructure using MRI and 2D relaxometry.

2 MATERIALS AND METHODS

2.1 Sample Preparation

Two different kinds of rheological foamed gel models have been prepared based on recipes formulated by SGGW (Poland) and IFR (England) respectively: the first one presented a formulation based on sugars and the second one was a sugarless composition.

2.1.1 Sugar Foamed Gel. Sugar foamed gel composition was 135 g of crystalline fructose, 45 g dextrose (crystalline glucose), 2.8 g agar-agar, 1.4 g albumin (from chicken egg white) and 140 ml distilled water.

The procedure used to prepare the foams was as follows: the distilled water was heated to 50°C and then agar powder was added. The mixture was agitated using an IKA stirrer at 100 rpm and heated to 90°C. The fructose plus glucose powder was dispersed in the hot agar solution, stirred (IKA stirrer, 200 rpm), and the mixture was brought to a boil to complete dissolution of sugar (temperature of solution 105 °C). Then, the solution was cooled in a bath to 50°C. The albumin was added and material was whipped using a kitchen mixer at 1400 rpm for 5 minutes and put it together in the other half of the syringe used previously to pour the sugarless foam.

2.1.2 Sugarless Foamed Gel. Sugarless foamed gel composition was 2.8 g of agarose (2%), 140 ml distilled water and 0.9996g (0.7%) Tween 60.

For the preparation of sugarless foams distilled water was added to the agarose powder and it was hand mixed. Then, it was heated in a microwave at 600W for 60 seconds, stirred and then heated again during 30 seconds. The Tween was mixed with a small amount of the dissolved agarose solution and added back to the bulk agarose solution. This step was repeated three times to remove any small Tween deposits. It was mixed with the agarose plus distilled water solution and mixed for 3 minutes. Afterwards, it was quenched in a melting ice bath for 1 hour and half of a 20 ml truncated syringe was filled with it.

At the end a syringe with two phases was obtained: one with the sugarless foam (from now NSF), which is placed above when the syringe is placed in a vertical position and the other one with the sugar foam (from now SF), which is in the top of the syringe when placed it in a vertical position. The syringe was covered with a film in order to protect it from the loss of moisture.

The foams were stored at 25°C during 2 hours before performing the MR experiments.

2.2 MR Equipment

All MR measurements were carried out on CAI of NMR (UCM) facilities on a Bruker BIOSPEC 47/40 (Ettlingen, Germany) spectrometer, working at 4.7T (200 MHz), equipped with a gradient system of 12 cm diameter, which generates 200 m/Tm gradients. For the transmission and reception a volume radiofrequency coil of 7 cm diameter was used. The bore of the magnet is horizontal, 147 cm long.

2.3 Texture Characterization

In order to measure the physical/textural attributes of the foamed gels, two different tests were performed in a TA.XTPlus Texture Analyser equipment: a penetration test following the standard Bloom method (British Standard BS757) and a confined compression test.
For both tests, cylindrical probes moved at a constant velocity of 0.5 $mm \cdot s^{-1}$ until a penetration/compression depth of 4 mm. For the penetration measurements, a cylindrical probe of Delrin® with a contact area of 126.68 mm^2, was forced into the sample formed in a cylindrical Simax ® glass container. The parameters used to describe the geometry of the measuring system are r= $6.35 \cdot 10^{-3}$m; R= $20 \cdot 10^{-3}$m; L= $25 \cdot 10^{-3}$m, being R the radius of the container (m), r the radius of the probe (m) and L the gel depth (m). The measured maximum penetration force F0(N) was used as “gel strength” and to calculate, following the method[21], the force corrected for buoyancy, Fcb(N), and the rheological parameter apparent Young´s modulus, Ye (Pa). To measure the resistance to compression stabilised foamed gels, formed into 20 ml teflon syringes with 19mm of inner diameter, were cut into

14mm (high) cylindrical probes and confined into a disk which had a hole of the probe size. Compression test was carried out using a 16mm diameter plunger. “Hardness” was defined as the maximum force (N) required to compress the sample[22], “adhesiveness” as the work to pull the probe away from the sample and calculated as the negative force area (N·mm) of the compression curve[23] and “plastic deformation” as permanent deformation after compression in mm.

2.4 MR Experiments

Macrostructure evolution of the samples was measured using Proton Density(DP) and T_2 maps. Figure 1 shows the time evolution of T2 and DP maps (11 out of 21 measurements, 1 hour delay between successive measurements). A clear evolution of T2 is found for foam 2 just underneath the interface. In the case of DP maps, a clear gradient is found for any time step and both foams. Besides for foam 1, a low DP area is found just above the interfaces which enlarge with time (Figure 1).

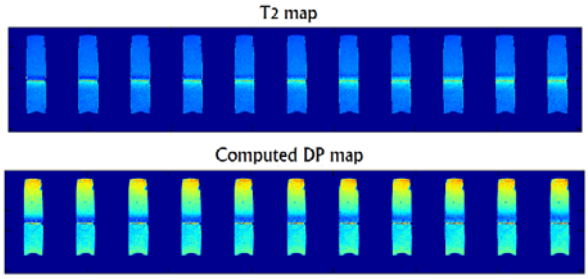

Figure 1 *T_2 and Proton Density maps of SF and NSF along 21 hours*

Microstructure evolution was monitored using ultrafast 2D relaxometry sequences, based on global and localized T1/T2 relaxation.

2.4.1 *Proton Density maps and T_2 maps.* Proton Density and T2 maps were obtained from a multiecho spin-echo series registered every hour during 21 hours. A total of 64 echoes with an echo time (TE) of 7.5 ms were acquired. The repetition time (TR) was set to 20 s in order to assure the complete longitudinal relaxation. The matrix size was 256x128 with a rectangular field of view (FOV) of 10x5 cm^2. The slice thickness was 5 mm. The intensity a T_2 maps were calculated using the ISA Tool of the ParaVision software (Bruker, Ettlingen, Germany).

2.4.2 *Global 2D relaxometry.* For global T1/T2 relaxometry, an inversion-recovery-CPMG sequence was used. 64 inversion steps were acquired with inversion times (TI) going from 0.5 ms to 20s in logaritmic scale. For each inversion step 64 echoes were achieved with (TE) of 4 ms. Global T1/T2 relaxometry was acquired every 30 minutes during 7 hours.

2.4.3 *Localized T1/T2 sequence.* For localized T1/T2 relaxometry spectra an inversion-recovery-CPMG with slice selection was used. A total of 11 axial slices with the same parameters as above were acquired.

2.5 Data Analysis

2.5.1 *Proton Density and T_2 maps.* The processing scheme followed was the same for both PD and T_2 maps. From the maps, the interface between both foams was

segmented and both foams separated in order to analyze them apart (Figure 2). On every map (T_2 and PD maps), each foam was divided into quadrants of 5 columns × 5 rows (25 quadrants per map), in order to have a high number of points per quadrant, approximately 2.000 2k points per quadrant. Then, the average, the variance and two first order moments (skewness and kurtosis) of the histogram of each quadrant were performed. Afterwards, the upper row of quadrants of the foam SF and the lower one of the foam NSF were deleted due to instability and in order to avoid the border effect, leaving 20 quadrants in each of the 21 maps. Then, an Analysis of Variance (ANOVA) was computed between every quadrant of each map (20 quadrants × 21 maps).

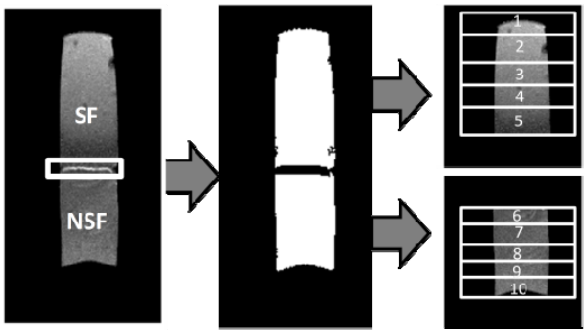

Figure 2 *Segmentation procedure performed on each of the PD and T_2 maps*

2.5.2 *Global 2D relaxometry and Localized 2D T1/T2 sequence.* Data were processed with Fast Inverse Laplace Transform[19].

3 RESULTS

3.1 Texture characterization

Both foams are significantly different in all the textural/rheological parameters considered. Results from Bloom Testing, performed on both foams on three consecutive days show that SF (dotted line) has significantly higher "gel strength" compared to NSF, and a different time evolution as well. On SF, the Force applied the third day (3.9N) was higher than the first one (3.2N) and nearly double that that of NSF. In both cases texture became harder in time (Figure 3). On the other hand, SF with a density of 647.58 $kg \cdot m^{-3}$ (±37.60) nearly double that that for NSF (364.45±36.62), shows, from the confined compression test, practically no permanent deformation (see Figure 3) along the evolution time, while NSF become less stable in time with a plastic deformation of 15.7% at day 2. SF shows too, significantly more adhesiveness than NSF which presents a value near to 0.

3.2 Macrostructure

PD and T2 maps for each Foamed Gel showed several differences in macrostructure and textural changes, during the evolution of the foam for 21 hours.

According to the Proton Density maps, on both Foam SF and Foam NSF significant differences between foam regions, as well as with time were found for average DP. On **Foam SF** spatial evolution might be seen in the region of study, as shown in Figure 1. The four regions of the foam have significant differences (F=7106.7). Furthermore, attending to the time, it is possible to find differences between the first time-step and the last one

corresponding to the Regions 4 and 5, which are the areas located on the bottom in the foam, near the interface. The interaction between time and region, thus, has significant differences with an F value of 31.208 (Table 1, Figure 4A) for **SF Foam**. Nevertheless, on **Foam NSF** significant differences between regions are achieved (F=189.52). Differences in the evolution of the latter are smaller than for **SF Foam** with an F value of 17.388. Interaction between spatial location in the foam and evolution in time did not show any significance (Figure 4B, Table 1) in this case, which means that DP evolution in time is similar for all regions in foam 2 (NSF).

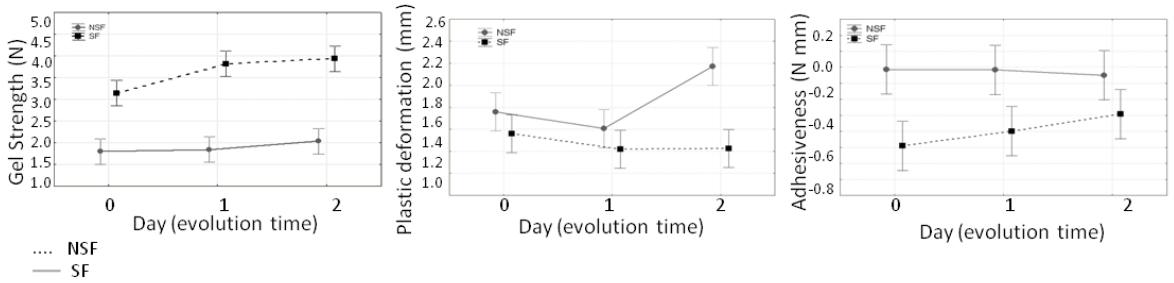

Figure 3 *Graphs of factorial ANOVA analysis results on "gel strength" parameter from Bloom test and "plastic deformation" and "adhesiveness" parameters extracted from confined compression test.*

Table 1 *Anova performed on DP and T2 Maps for sugar and sugarless foams (SF and NSF respectively): ** 1% significance level, * 5% significance level*

	Foam SF DP	Foam NSF DP	Foam SF T2	Foam NSF T2
Source	Fisher value	Fisher value	Fisher value	Fisher value
Time	89.034 **	17.388 *	19.834 **	13.232 **
Region	7106.7 **	189.52 **	586.02 **	4899.9 **
Interaction	31.208 **	0.07273 ^{ns}	96.345 **	33.699 **

In relation with T_2 maps textural changes are reflected by the average and by the variance within each region. On **Foam SF**, the averages have significant differences related to time (F=19.834), region (F=586.02) and in the interaction of both factors (F=96.345) (Table 1, Figure 4C). Region differences are particularly visible on both Regions 4 and 5, that are located on the bottom of the foam and thus, near the interface, which suffers the larger changes and water migration. Variance showed differences also in groups near to the interface (4 and 5), which explained the instability of this area (Figure 5A). For **Foam NSF**, T2 average presented significant differences between regions (F=4899.9), specially on that near the interface (Region 6). Also, evolution of the texture occurs with time (F=13.232) and in the interaction of these two factors (F=33.699) (Figure 4D). Related to variance, higher differences are seen in the two groups which are nearer to the interface (Figure 5B). Also higher variance within regions is found for **NSF Foam** compared to **SF Foam**, this fact can be related to the higher pore size of **NSF Foam**, which is at the spatial resolution limit and so can also be detected by such textural change. Variance for NSF nearly doubles that of SF, higher variance relates to higher pore size (at MRI spatial resolution level) for NSF while smaller pore size (below MRI resolution level) is found for SF, that is more homogeneous gray level in the quadrant.

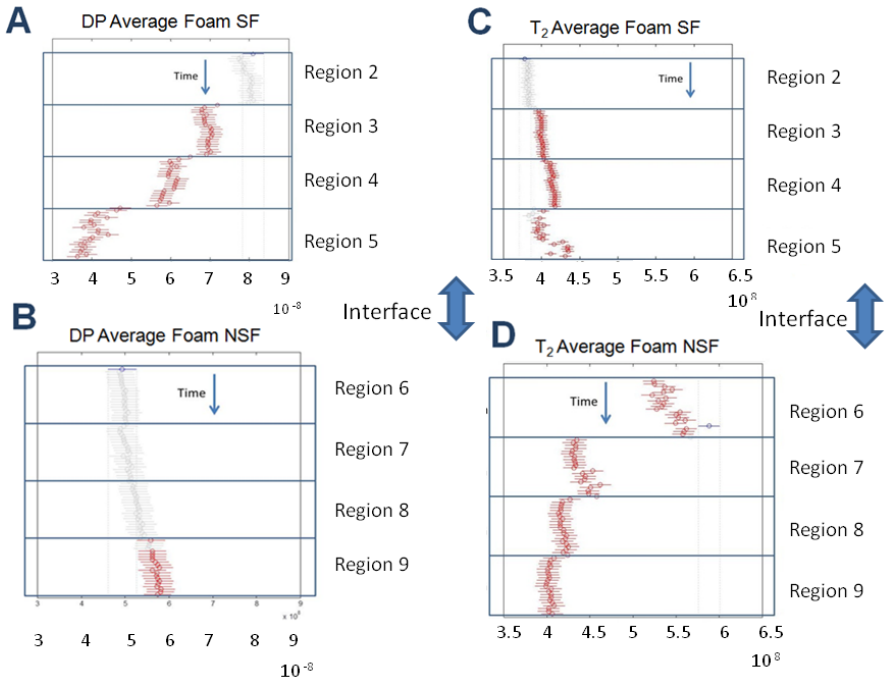

Figure 4 *ANOVA performed on the DPand T2 maps: average of the regions along time (21 hours). A. ANOVA on SF on DP average; B. ANOVA on NSF on DP average. C. ANOVA on SF on T2 average; D. ANOVA on NSF on T2 average*

3.3 Microstructure

3.3.1 Global 2D relaxometry. Using Global 2D T1/T2 relaxometry both foams were differentiated and microscopic changes were observed. In Figure 6, differences between the different pore size and the microstructure evolution after 21 hours is observed as a consequence of the free water redistribution through larger pores and to capillarity phenomena in smaller pores between both foams.

3.3.2 Localized 2D relaxometry. Localized 2D T1/T2 sequences provide a significant change in the fingerprint compared to Global 2D relaxometry. The smaller the slice the more homogeneous the parameters for each foams seem, which is consistent with the gradient found in the T2 Maps; only the interface highlights the existence of free water and the coexistence of several structures (Figure 7).

4 CONCLUSIONS

MRI is a successful tool to detect textural differences even though the pores are not visible in the image or the map. It can also address water migrations and thus, it is possible to performe of region-temporal analysis in order to assess the food evolution.

Global 2D T1/T2 relaxometry allows the identification of microscopic differences between both foams but may lose its usefulness when very high heterogeneity and gradients within samples are found.

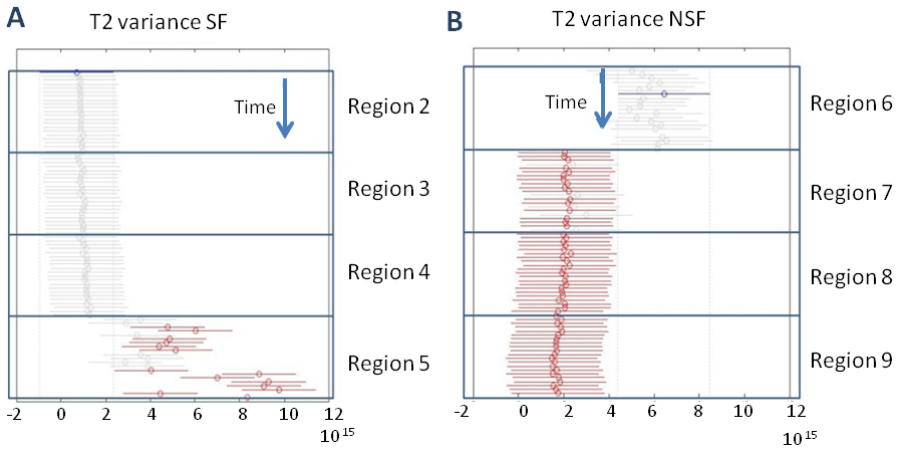

Figure 5 *ANOVA performed on the T2 maps: variance of the regions along time (21 hours). A. ANOVA on SF on T2 variance; B. ANOVA on NSF on T2 variance within region.*

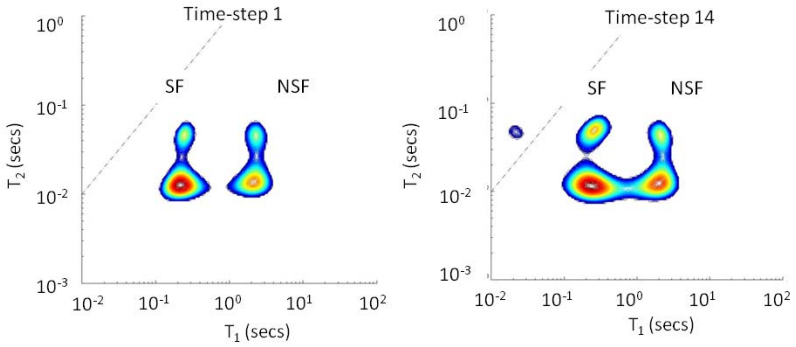

Figure 6 *2D T1/T2 relaxometry. A. Initial moment; B. After 21 hours. The Areas with large T1 correspond to NSF foams, while lower values of T1 refer to SF foam. On the other hand large T2 refers to larger pores, while lower T2 may be caused by smaller pores. Water exchange between both foams is clear at the end of the 21h period according to Global 2D relaxometry.*

2D localized relaxometry can successfully select areas of study so that local evolution can be examined by further study, and proper identification and classification of structuresmay be performed with higher reliability. It is important to state that Global 2D relaxometry is not simply an addition of the local regions which makes it more difficult to interpret the Global features.

Acknowledgements

This publication has been produced with the financial support of the European Union (project FP7-226783 - InsideFood). The opinions expressed in this document do by no means reflect the official opinion of the European Union or its representatives.

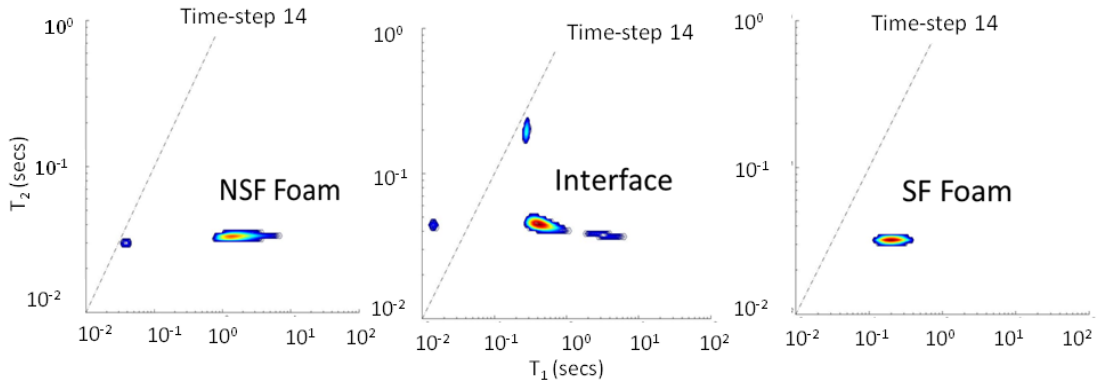

Figure 7 *2D T1/T2 Localized relaxometry on the Sugarless Foam (NSF), the Interface and the Sugar Foam (SF)*

References

1 B.P. Hills, C.E. Manning, Y. Ridge and T. Brocklehurst, *J Sci Food Agr*, 1996, **71**, 185.
2 E. Vittadini, P. Chinachoti, J.P. Lavoie and X. Pham, *Inn Food Sci Emerg Technol*, 2005, **6**, 21.
3 J.M. Aguilera, *J Food Eng*, 2005, 67, 3.
4 P.J. Lillford, *J. Texture Stud*., 2011, 42, 130.
5 J. Parada and J.M. Aguilera, *J Food Sci*, 2007, 72, R21.
6 P. Lopez-Sanchez, J. Nijsse, H.C.G. Blonk, L. Bialek, S Schumm and M. Langtom, 2011, *J Sci Food Agr*, 91, 207.
7 L. Seguí, P.J. Fito and P. Fito, *J Food Eng*, 2011, 110, 240.
8 V. De Smedt, E. Pauwels, J. De Baerdemaeker and B. Nicolai, *Post Biol and Tech*, 1998, 14, 151.
9 H.K. Mebatsion, P. Verboven, B.E. Verlinden, Q.T. Ho, T.A. Nguyen and B.M. Nicolai, *Computers & electronics in agriculture*, 2006, **52**, 36.
10 F. Mendoza, P. Verboven, H.K. Mebatsion, G. Kerckhofs, M. Wevers and B. Nicolai, *Planta*, 2007, **226**, 559.
11 P. Verboven, G. Kerckhofs, H.K. Mebatsion, Q.T. Ho, K. Temst, M. Wevers, P. Cloetens and B. Nicolai, *Plant Physiol*, 2008, **147**, 518.
12 F. Mendoza, P. Verboven, Q.T. Ho, G. Kerckhofs, M. Wevers and B. Nicolai, *J Food Eng*, 2010, **99**, 206.
13 P. Frisullo, M. Barnabà, L. Navarini and M.A. Del Nobile, *J Food Eng*, 2012, **108**, 232.
14 M. Musse, F. De Guio, S. Quellec, M. Cambert, S. Challois and A. Davenel, *Magn Reson Imaging*, 2012, **28**, 1525.
15 A.M. Haiduc and J. Van Duynhoven, *Magn Reson Imaging*, 2005, **23**, 343.
16 N. Marigheto, L. Venturi and B. Hills, *Post Biol and Tech*, 2008, **48**, 331.
17 L. Zhang and M.J. McCarthy, *Post Biol and Tech*, 2012, **67**, 96.
18 L. Venturi, J. Warner and B. Hills, *Magn Reson Imaging*, 2010, **28**, 964.
19 L. Venturi and B. Hills, *Magn Reson Imaging*, 2010, **28**, 171.
20 Y.Q. Song and L. Venkataramanan, M.D. Hurliman, M. Flaum, P. Frulla and C. Straley, *J. Magn.Reson*, 2002, **154**(2).
21 C.M. Gregson, S.E. Hill, J.R. Mitchell and J. Smewing, *J. Carbohydr. Polym*, 1999, **38**, 255.
22 L. Vazquez-Araujo, A. Verdu, R. Murcia, F. Burlo and A.A. Carbonell-Barrachina, *J. Texture Stud.*, 2006, **37**, 63.
23 M.C. Nunes, A. Raymundo and I. Sousa, *J. Food Hydrocolloids*, 2006, **71**, 185.